Earthline Journal of Chemical Sciences
E-ISSN: 2581-9003; CODEN: EJCSB4
Volume 11, Number 3, 2024, Pages 385-404
https://doi.org/10.34198/ejcs.11324.385404

Dinitro-[1H,4H]-dihydropyrazines - A DFT treatment

Lemi Türker

Department of Chemistry, Middle East Technical University, Üniversiteler, Eskişehir Yolu No: 1, 06800 Çankaya/Ankara, Turkey; e-mail: lturker@gmail.com; lturker@metu.edu.tr

Abstract

Dinitro-(1H,4H)-dihydropyrazine isomers and the 1,3- and 1,5-proton tautomers of these isomers are considered within the constraints of density functional theory at the level of B3LYP/6-311++G(d,p). All the structures are electronically stable, thermodynamically exothermic and have favorable Gibbs' free energy of formation values at the standard states. Various quantum chemical properties, including IR and UV-VIS spectra, the HOMO and LUMO energies etc., have been obtained and discussed. The NICS values have been calculated for the antiaromaticity order of the isomers considered.

1. Introduction

The lH,4H-dihydropyrazine ring system is an interesting conjugated cyclic structure containing 8π-electrons. It is electronically analogous to cyclooctatetraene and la-azepine, both of which have in recent years displayed some fascinating chemistry [l,2]. For leading information, one should refer to references [2,3].

Chen and Fowler [3] reported the correct structure which is in accordance with the data given by Mason and Winder [4]. Some analogues of the 1,4-dihydropyrazine were synthesized by Brook and coworkers [5]. Preparation of stable 1,4-dihydropyrazines were considered by Fourrey [6]. Pyrazines which are known to be formed during food processing *via* Maillard-type reactions have received considerable attention because of their potent flavoring properties [7]. The recent status of pyrazinacenes chemistry was presented by Richards and Hill [8]. Lown *et al*., investigated the stereochemistry and mechanism of the thermal [1,3] alkyl shift of stable 1,4-dialkyl-1,4-dihydropyrazines [9].

Received: May 16, 2024; Accepted: June 18, 2024; Published: June 26, 2024

Keywords and phrases: dihydropyrazine; dinitro-dihydropyrazines; density functional; isomers; explosives; NICS.

Some 1,4-dihydropyrazines exhibit remarkable biological effects [10,11] such as DNA strand-breakage activity [11] or mutagenesis [12]. In the work of Takechi, *et al*., dihydropyrazine (DHP), which induces mutagenesis in *E. coli*, was investigated [12].

On the other hand, density functional theory (DFT) calculations at M06L/6-311++G(d,p) level have been carried out on 24 dihydropyrazine annulated linear polyacene systems to study their aromaticity and HOMO-LUMO energy gap [13].

Sun *et al*., concentrated on the intriguing tautomerism behaviors of a new hexazapentacene derivative, named DHHAP [14]. In solution, DHHAP exists as a mixture of benzenoid and quinonoid tautomers in a rough ratio of 1 : 1. DFT calculations reveal that DHHAP is slightly more stable than its $4n + 2\pi$ hexazapentacene counterpart although it has $4n\ \pi$ electrons. DHHAP exhibits different halochromic behaviors upon addition of strong and mild acids [14].

Vlček and coworkers considered a set of twenty molecules containing 1,4-dihydro- or tetrahydropyrazine ring and they calculated using *ab initio* methods. This set also includes previously prepared diacetyl- or disilyldihydropyrazines. On the basis of structural, electronic and energy arguments it was proposed to classify 1,4-dihydropyrazines as nonaromatic compounds [15].

In the present study, isomers of dinitro-(1H,4H)-dihydropyrazine and their 1,3- and 1,5-proton tautomers were considered within the limitations of the density functional theory (DFT).

2. Method of Calculations

In the present study, the initial structural optimizations of all the structures leading to energy minima have been achieved by using MM2 method followed by semi-empirical PM3 self-consistent fields molecular orbital (SCF MO) method [16,17] at the restricted level [18,19]. Subsequent optimizations were achieved at Hartree-Fock level using various basis sets. Then, the structural optimizations were managed within the framework of density functional theory (DFT) [20,21] at the level of B3LYP/6-311++G(d,p) [19,22]. The exchange term of B3LYP consists of hybrid Hartree-Fock and local spin density (LSD) exchange functions with Becke's gradient correlation to LSD exchange [21,23]. The correlation term of B3LYP consists of the Vosko, Wilk, Nusair (VWN3) local correlation functional [24] and Lee, Yang, Parr (LYP) correlation correction functional [25]. Also, the vibrational analyses have been done. The total electronic energies are

corrected for the zero point vibrational energy (ZPE). The normal mode analysis for each structure yielded no imaginary frequencies for the 3*N*–6 vibrational degrees of freedom, where *N* is the number of atoms in the system. This indicates that the structure of each molecule corresponds to at least a local minimum on the potential energy surface. All these calculations were done by using the Spartan 06 package program [26]. Whereas the nucleus-independent chemical shift, NICS(0), calculations have been performed by using Gaussian 03 program [27].

3. Results and Discussion

Isomers of dinitro-[1H,4H]-dihydropyrazines

Figure 1 shows the optimized structures of the isomers considered (top and side views). It shows the direction of the dipole moment vectors as well. As seen in the figure, except the case of isomer-B1, the others possess a nonplanar ring system. The ring in B1 is coplanar with the nitro groups.

Table 1 displays some calculated properties of the isomers considered. Note that isomer-B1 is highly symmetrical, possesses point group of C_i thus its dipole moment vector is zero. The other isomers have C_1 point group.

On the other hand, the polarizability is defined according to the multivariable formula [26].

$$\text{Polarizability} = 0.08*V - 13.0353*h + 0.979920*h^2 + 41.3791$$

where V and h are the Van der Waals volume and hardness, respectively. Hardness is defined as,

$$\text{Hardness} = -(\varepsilon_{HOMO} - \varepsilon_{LUMO})/2$$

where ε_{HOMO} and ε_{LUMO} are the molecular orbital energies of the highest occupied (HOMO) and the lowest unoccupied (LUMO) molecular orbital energies, respectively.

It is worth mentioning that the polar surface area (PSA) is defined as the amount of molecular surface area arising from polar atoms (N,O) together with their attached hydrogen atoms.

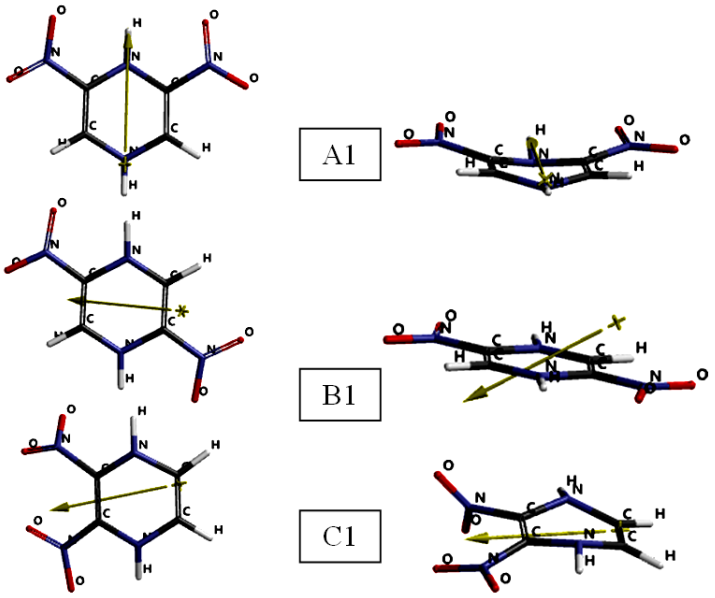

Figure 1. Optimized structures of the isomers considered.

Table 1. Some calculated properties of the isomers considered.

Isomers	Dipole Moment (Debye)	Polarizability	Area (Å²)	Volume (Å³)	PSA (Å²)
A1	6.96	51.72	162.56	134.78	99.856
B1	0.00	51.67	162.52	134.62	98.357
C1	6.83	51.79	162.90	135.19	99.716

Polarizabilities in 10^{-30} m^3 units. All have the ovality value of 1.28

Note that all the isomers considered have negative log P values. It is worth mentioning that a negative value for log P means the compound has a higher affinity for the aqueous phase (it is more hydrophilic); when log P = 0 the compound is equally partitioned between the lipid and aqueous phases; a positive value for log P denotes a higher concentration in the lipid phase (i.e., the compound is more lipophilic).

Table 2 shows aqueous and solvation energies of the isomers considered. The solvation energy data are based on SM5.4/A model [26]. The data in the table indicate that isomer-B1 is solvated better than the others and the order of solvation is B1>A1>C1.

The order should arise mainly from the charge distribution in B1 in spite of the fact that it possesses no resultant dipole moment. Also note that in all these isomeric compounds the ring nitrogen atoms take the role of hydrogen bond acceptor and donor while the nitro groups act as hydrogen bond acceptor.

Table 2. Aqueous and solvation energies of the isomers.

Isomers	E_{aq}	Solvation E
A1	-1771460.30	-49.09
B1	-1771483.14	-50.66
C1	-1771372.27	-27.57

All have the Log P value of -2.71. Energies in kJ/mol.

Figure 2 stands for the calculated IR spectra of the isomers. As seen in the figure, isomer-B1 has only a single N-H stretching due to the symmetry whereas the others have two above 3500 cm^{-1}. Note that the symmetry highly simplifies the spectrum of B1 as compared to the others.

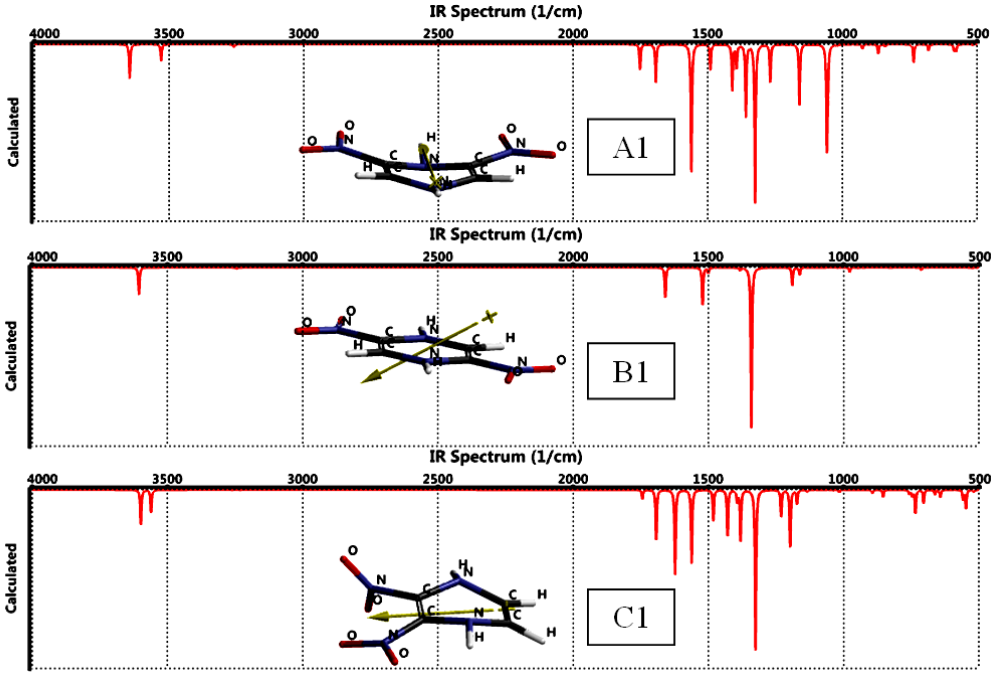

Figure 2. Calculated IR spectra of the isomers considered.

Figure 3 shows the electrostatic potential charges (ESP) on the atoms of the isomers. Note that the ESP charges are obtained by the program based on a numerical method that generates charges that reproduce the electrostatic potential field from the entire wavefunction [26]. Obviously, distribution of the charges is dictated by the position of the nitro groups, not only the absolute magnitude but also the kind. For instance, the partial charges on carbon atoms linked to the nitro groups are positive in isomer-A1 but are negative in C1.

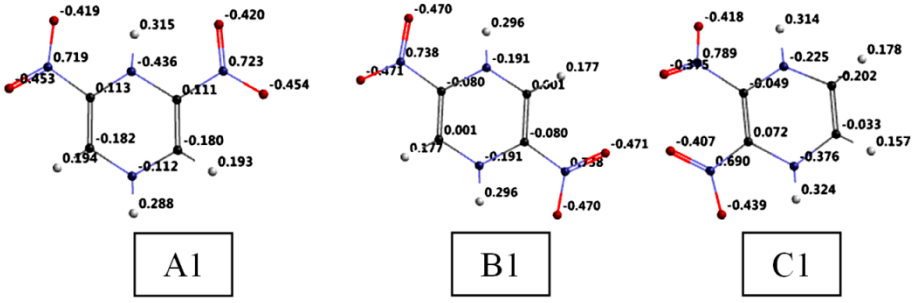

Figure 3. Electrostatic charges on the atoms of the isomers.

Figure 4 shows the electrostatic potential maps of the isomers considered where negative potential regions coincide with red/reddish and positive ones with blue/bluish parts of the maps.

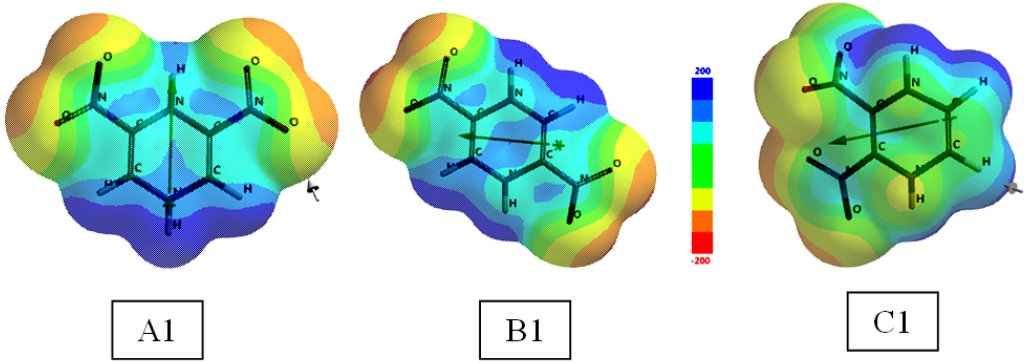

Figure 4. Electrostatic potential maps of the isomers.

Table 3 shows some of the standard thermo chemical formation data of the isomers considered. The data reveal that formations of all the isomers are exothermic and favored. The orders of Hº and Gº values are the same and follows the algebraic order of

B1<A1<C1. Thus, B1 is the most exothermic and most favored whereas C1 is the least exothermic and least favored one. Entropically the order of favorability is B1>C1>A1 which should arise from the relative positions and conformations of the nitro groups.

Table 3. Some thermo chemical values of the isomers considered.

Isomers	Hº	Sº (J/molº)	Gº
A1	-1771129.762	388.86	-1771245.703
B1	-1771151.617	392.93	-1771268.771
C1	-1771064.460	389.80	-1771180.679

Energies in kJ/mol.

Table 4 shows some energies of the isomers considered where E, ZPE and E_C stand for the total electronic energy, zero point vibrational energy and the corrected total electronic energy, respectively. As the data reveal, all of the structures are electronically stable and the order is B1>A1>C1>. Thus isomer-B1 is thermo chemically and electronically more favored over the others. The steric and electronic factors should be responsible for that which should be governed by some symmetry properties.

Table 4. Some energies of the isomers considered.

Isomers	E	ZPE	E_C
A1	-1771411.20	272.11	-1771139.09
B1	-1771432.48	270.91	-1771161.57
C1	-1771344.70	270.61	-1771074.09

Energies in kJ/mol.

Table 5 shows the HOMO, LUMO energies and the interfrontier molecular orbital energy gaps (Δε) of the isomers considered, where $\Delta\varepsilon=\varepsilon_{LUMO}-\varepsilon_{HOMO}$. The HOMO energies follow the algebraic order of B1<A1<C1. The LUMO energy order is C1<A1<B1. Consequently, the order of Δε values becomes B1>A1>C1.

Note that the impact sensitivity of explosives are related to the interfrontier molecular orbital energy gap values. That is narrower the gap, the explosive becomes more sensitive to an impact stimulus [28,29]. Thus C1 is expected to be the most sensitive to impact among the others.

Table 5. The HOMO, LUMO energies and Δε values of the isomers considered.

Isomers	HOMO	LUMO	Δε
A1	-589.67	-348.34	241.33
B1	-590.37	-334.33	256.04
C1	-574.95	-350.00	224.95

Energies in kJ/mol.

Figure 5 stands for the time-dependent density functional UV-VIS spectra of the isomers. As seen in the figure, variation of positions of the nitro groups has some influence on the spectra. The highly striking bathochromic effect in the cases of A1 and C1 in contrast to B1 is noticeable. Note that these isomers may exhibit push-pull type resonance, and the extend of the conjugation should dictate the degree of the bathochromic effect. Since Δε values of A1 and C1 are smaller than B1, then isomer-B1 is expected not to exhibit any appreciable degree of bathochromic effect compared to A1 and C1.

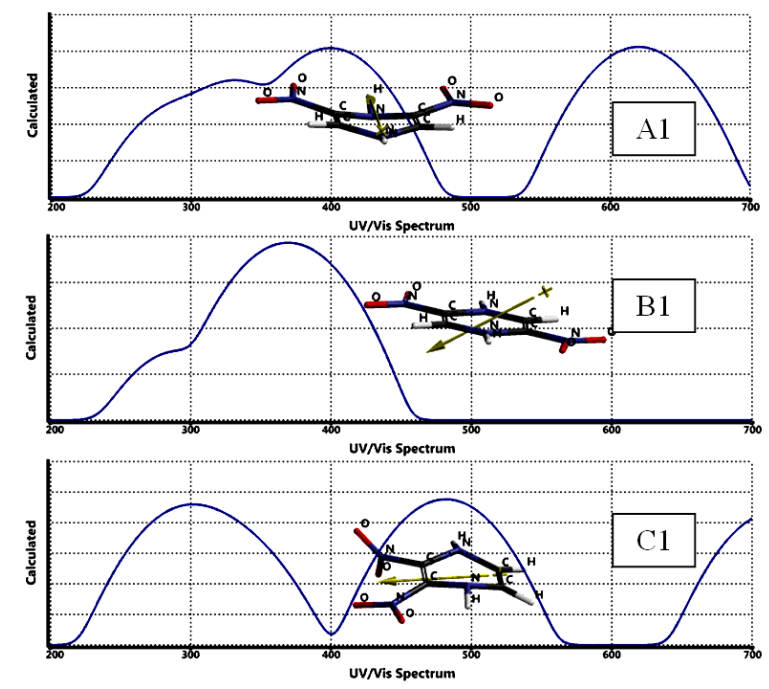

Figure 5. The time-dependent density functional UV-VIS spectra of the isomers.

Figure 6 shows the local ionization potential maps of the isomers considered where conventionally red/reddish regions (if any exists) on the density surface indicate areas from which electron removal is relatively easy, meaning that they are subject to electrophilic attack.

Figure 7 displays the LUMO maps of the isomers considered. Note that a LUMO map displays the absolute value of the LUMO on the electron density surface. The blue color (if any exists) stands for the maximum value of the LUMO and the red colored region, associates with the minimum value. Note that the LUMO and NEXTLUMO are the major orbitals directing the molecule towards of the attack of nucleophiles. Positions where the greatest LUMO coefficient exists is the most vulnerable site in nucleophilic reactions.

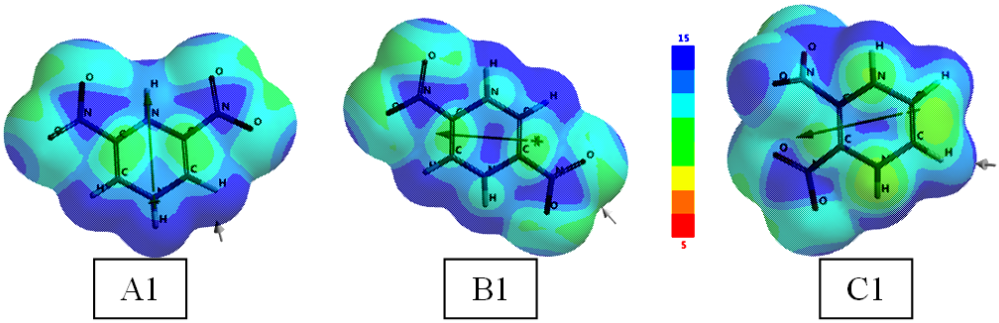

Figure 6. The local ionization potential maps of the isomers.

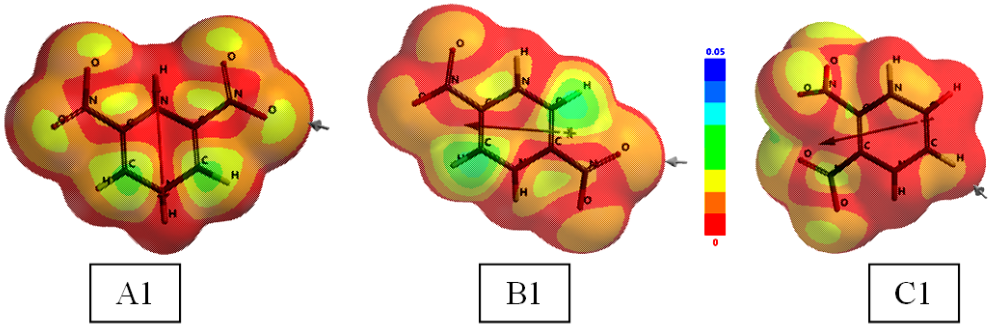

Figure 7. The LUMO maps of the isomers.

NICS

To get an idea about the antiaromaticity order of the dihydropyrazine ring present in the isomers considered, "nucleus-independent chemical shift" (NICS) values were

obtained. Note that NICS is the computed value of the negative magnetic shielding at some selected point in space, generally at center of a ring or cage [30-42]. There are many review articles about NICS [34,35,41,42]. The calculated data so far have piled in the literature [30-42], have indicated that negative NICS values are associated with aromaticity. On the contrary, positive NICS values are associated with antiaromaticity while small NICS values are indicative of non-aromaticity. However, it is to be mentioned that although NICS approach has been proved to be an effective probe for the local aromaticity of individual rings of polycyclic systems a couple of contradictory results have been reported [39]. Table 6 shows the NICS(0) values of the isomers considered. Note that the ring system of these dihydropyrazines possesses 8π-electrons and except B1 isomer, the others are not coplanar.

Table 6 shows the NICS(0) values of dinitro-dihydropyrazines considered. As seen in the table, all the isomers considered are characterized with antiaromaticity. However, based on the NICS(0) values the antiaromaticity order is C1<A1<B1. Since B1 isomer is a coplanar system among the isomers (see Figure 1), it suffers from 8π-electron ownership mostly. The study of Vlček, and coworkers indicated that structures of 1,4-dihydropyrazine derivatives are strongly dependent on ring substituents and change from planar to heavily distorted boat conformations [15]. In the planar and near-planar structures of some 1,4-diacyl- or 1,4-diformyl-1,4-dihydropyrazines, conjugation of nitrogen lone pairs and ring bond π- electrons is small.

Table 6. The NICS(0) values of dinitro-[1H,4H]-dihydropyrazines considered.

A1	B1	C1
10.4968	15.3760	6.1036

Some tautomers of dinitro-[1H,4H]-dihydropyrazines

Dinitro-dihydropyrazines may exhibit 1,3- or 1,5-type proton tautomerism. The hydrogens linked to ring nitrogens participate the process and shift to nitro oxygens or to ring carbons. Note that substances which are isomeric under certain conditions are tautomeric under more drastic conditions [43,44]. Figure 8 shows the optimized structures of those tautomers. Note that tautomers derived from A1-isomer are labeled as A2, A3 etc. A similar notation has been followed for tautomers from isomers B1 and C1 (see Figure 1 for the structures of parent isomers A1, B1 and C1). Note that directions of the dipole moment vectors change as proton moves from one site to other. Also note that

tautomers considered, involve nitrogen to oxygen (oxygen of the nitro group) tautomeric shift in 1,5-type tautomers whereas nitrogen to carbon shift in the 1,3-type tautomers.

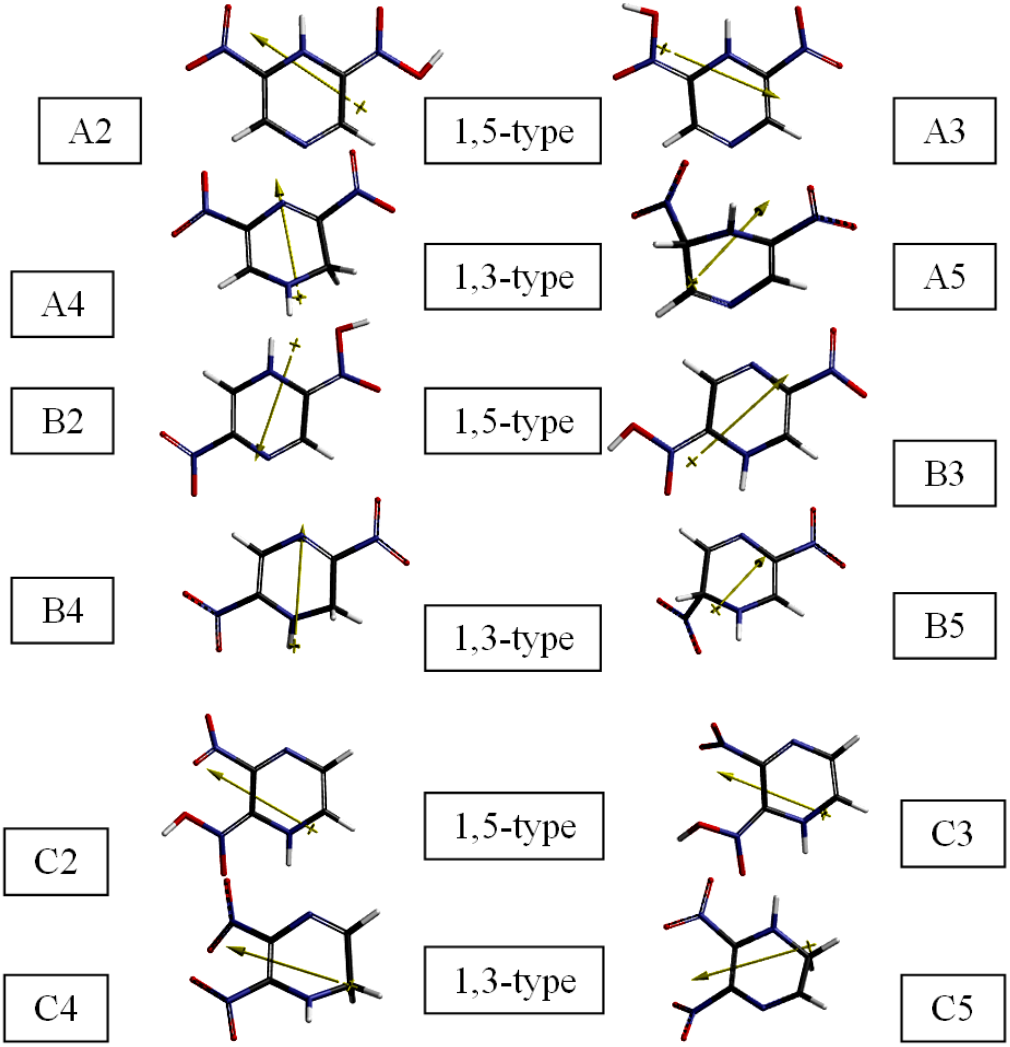

Figure 8. Optimized structures of the tautomers considered.

Although, some of the tautomer structures in 2-dimentional space seem to be symmetrically interrelated with each other, in fact in 3-dimentional space (optimized structures) they exhibit some differences.

Table 7 shows some of the thermo chemical data of the tautomers considered. The data reveal that formations of the tautomers are exothermic and thermodynamically

favored. Algebraic order for H^o values group wise are A5<A4<A2<A1<A3; B1<B5<B3<B2<B4; C2<C3<C5<C4<C1. The same order holds for G^o values of A and C series of structures whereas for B series the order of G^o values becomes B1<B3<B5<B4<B2. As seen in Table 7 some 1,3-type tautomers in the same group are more exothermic and more favored than 1,3-type even the parent structures (e.g., A5 and A1, A4 and A3). In some cases 1,5 type is more exothermic and favored than 1,3 type (e.g., B2 and B4; C2 and C4).

Table 7. Some thermo chemical properties of the tautomers considered.

Tautomer	Type of tautomeric shift	H^o	S^o (J/mol^o)	G^o
A1		-1771129.762	388.86	-1771245.703
A2	1,5	-1771133.262	398.66	-1771252.125
A3	1,5	-1771125.414	398.37	-1771244.190
A4	1,3	-1771138.353	387.39	-1771253.855
A5	1,3	-1771141.777	385.93	-1771256.843
B1		-1771151.617	392.93	-1771268.771
B2	1,5	-1771138.232	396.01	-1771256.305
B3	1,5	-1771148.886	396.36	-1771267.064
B4	1,3	-1771122.860	388.58	-1771238.716
B5	1,3	-1771151.139	386.86	-1771266.481
C1		-1771064.460	389.80	-1771180.679
C2	1,5	-1771108.537	396.11	-1771226.636
C3	1,5	-1771108.333	395.03	-1771226.111
C4	1,3	-1771085.703	388.78	-1771201.618
C5	1,3	-1771085.879	389.19	-1771201.919

Energies in kJ/mol.

In A-series of structures 1,3-type tautomer is the most exothermic and favored one, whereas in C-series 1,5-tautomer gets the priority.

Table 8 shows some energies of the tautomers considered. As defined previously E, ZPE and E_C stand for the total electronic energy, zero point vibrational energy and the corrected total electronic energy, respectively. As the data reveal, all of the structures are electronically stable. As seen in the table the electronic stability of the structures (in vacuum) is highly related to specific tautomeric form. In some cases, the tautomer is more stable than its parent structure.

Table 8. Some energies of the tautomers considered.

Tautomer	Type of tautomeric shift	E	ZPE	E_C	E_{aq}	E_{solv}
A1		-1771411.20	272.11	-1771139.09	-1771460.30	-49.09
A2	1,5	-1771411.20	267.22	-1771143.98	-1771445.54	-34.34
A3	1,5	-1771402.85	266.72	-1771136.13	-1771429.56	-26.71
A4	1,3	-1771420.13	272.86	-1771147.27	-1771476.82	-56.69
A5	1,3	-1771422.93	272.34	-1771150.59	-1771465.72	-42.78
B1		-1771432.48	270.91	-1771161.57	-1771483.14	-50.66
B2	1,5	-1771417.97	269.27	-1771148.70	-1771465.13	-47.16
B3	1,5	-1771428.43	269.16	-1771159.27	-1771474.11	-45.68
B4	1,3	-1771403.42	271.37	-1771132.05	-1771422.88	-19.46
B5	1,3	-1771432.74	272.75	-1771159.99	-1771493.01	-60.27
C1		-1771344.70	270.61	-1771074.09	-1771372.27	-27.57
C2	1,5	-1771388.40	269.43	-1771118.97	-1771433.32	-44.92
C3	1,5	-1771388.42	269.64	-1771118.78	-1771433.53	-45.11
C4	1,3	-1771366.04	271.00	-1771095.04	-1771408.93	-42.89
C5	1,3	-1771366.08	270.81	-1771095.27	-1771408.85	-42.77

Energies in kJ/mol.

Table 8 reveals that the algebraic order of E values (group wise) is A5< A4< A1=A2<A3; B5< B1<B3< B2< B4 and C3< C2< C5< C4<C1, whereas E_C values follow the order of A5< A4< A2< A1< A3; B1< B5< B3< B2< B4 and C2< C3< C4< C5< C1. So, A5, B1 and C2 are electronically the most stable structures within their groups. The stability is dictated by various factors including steric and electronic factors.

The table also shows the aqueous energies of the tautomers which have the order of A4< A5< A1< A2< A3; B5< B1< B3< B2< B4; C3< C2< C4< C5< C1. The solvation energy data (SM5.4/A model [26]) in the table gives the algebraic order of the solvation energies as A4< A1< A5< A2< A3; B5< B1< B2< B3< B4; C3< C2< C4< C5< C1. The data in the table indicate that tautomers-A4, B1 and C2 are solvated better than the others in their groups. The order should arise mainly from the charge-charge, charge-dipole and/or dipole-dipole interactions. Also note that in all these isomeric/tautomeric compounds the ring nitrogen atoms take the role of hydrogen bond acceptor and donor while the nitro groups act as hydrogen bond acceptor. Note that A5,B1 and C2 are thermo chemically more favored and most stable tautomers among their groups (see Tables 7 and 8). In all the tautomers considered, B1 (a parent structure) is the most favorable and stable one.

Table 9 shows the HOMO, LUMO energies and the interfrontier molecular orbital energy gaps $\Delta\varepsilon$ (defined as $\Delta\varepsilon=\varepsilon_{LUMO}-\varepsilon_{HOMO}$) of the tautomers considered. The algebraic order of HOMO energies (group wise) is A5< A4< A1< A2<A3; B5< B4< B3< B2< B1; C4< C5< C3< C2< C1. Whereas, the LUMO energy order is A3< A2< A5< A4< A1; B4< B1< B2< B3< B5; C4< C5< C1< C2< C3. Consequently, the order of interfrontier molecular orbital energy gap happens as A4> A5> A1> A2> A3; B5> B3> B2> B4> B1; C4> C5> C3> C2> C1. Of course, the HOMO and LUMO orders are dictated by the positions of the nitro groups in each group of isomers and their tautomers as well as the π-electron conjugation. Note that any electron donating effect raises up the HOMO and LUMO energies whereas electron acceptors lower both the frontier molecular orbital energies. Any extended conjugation lowers the LUMO but raises up the HOMO energy level [45]. Consequently, $\Delta\varepsilon$ values are dictated by all these factors.

Figure 9 shows the time-dependent density functional UV-VIS spectra of the most favorable and stable tautomers within each group. However, most of them also stand for representatives of each group. In the cases of A- and B-types, the spectra are mostly similar to each other but in some C-types appreciable bathochromic shift occurs in to the visible part of the spectrum.

Table 9. The HOMO, LUMO energies and Δε values of the tautomers considered.

Tautomer	Type of tautomeric shift	HOMO	LUMO	Δε
A1		-589.67	-348.34	241.33
A2	1,5	-586.57	-372.73	213.84
A3	1,5	-581.48	-376.91	204.57
A4	1,3	-707.36	-355.41	351.95
A5	1,3	-716.07	-365.44	350.63
B1		-590.37	-334.33	256.04
B2	1,5	-596.86	-291.31	305.55
B3	1,5	-601.73	-290.70	311.03
B4	1,3	-704.63	-405.84	298.79
B5	1,3	-716.82	-282.90	433.92
C1		-574.95	-350.00	224.95
C2	1,5	-581.16	-299.15	282.01
C3	1,5	-581.20	-298.78	282.42
C4	1,3	-700.81	-373.47	327.34
C5	1,3	-700.20	-373.32	326.88

Energies in kJ/mol.

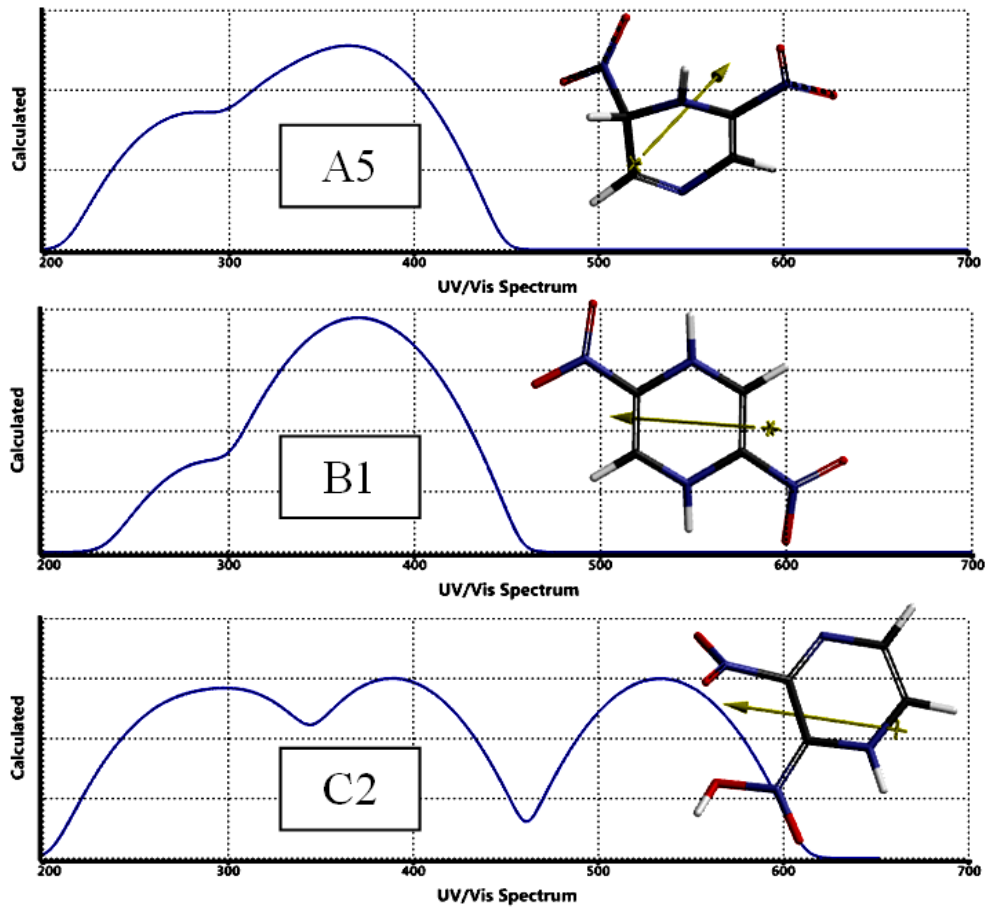

Figure 9. The calculated UV-VIS spectra of some of the tautomers.

4. Conclusion

The present study within the restrictions of density functional theory and the level of basis set employed has revealed that all the structures considered possess thermo chemically favorable values and they are electronically stable. In some cases the tautomer is more favored and more stable than the parent structure considered. The properties of these structures are dictated by the electronic and steric factors. The relative positions of the nitro groups on the ring in the parent structures should be the dominant factor which have pronounced effects on properties of the tautomers.

References

[1] Paquette, L.A., Kuhls, D.E., Barrett, J.H., & Leichter, L.M. (1969). Unsaturated heterocyclic systems. LV. Cycloaddition reactions of derivatives of 1H-azepine. *J. Org. Chem*., *34*, 2888-2896. https://doi.org/10.1021/jo01262a018

[2] Schroder, G. (1956). *Cyclooctatetraene*, Weinheim/Bergstr., Germany: Verlag Chemie.

[3] Chen, S-J, & Fowler, F.W. (1970). Structures of alleged 1,4-dihydropyrazines. *J. Org. Chem., 56*(11)*,* 3987- 3989. https://doi.org/10.1021/jo00836a100

[4] Mason, A.T., & Winder, G.R. (1893). Syntheses of piazine derivatives. Interaction of benzylamine and phenacyl bromide. *J. Chem. Soc., 63*, 1355-1375. https://doi.org/10.1039/ct8936301355

[5] Brook, D.J.R., Noll, B.C., & Koch, T.H. (1998). Carbonyl and thiocarbonyl stabilized 1,4-dihydropyrazines: synthesis and characterization. *J. Chem. Soc., Perkin Trans. 1,* 289-292. https://doi.org/10.1039/A705391F

[6] Fourrey, J-L. (1987). Preparation of stable 1,4-dihydropyrazines. *J. Chem. Soc. Perkin Trans. I*, 1841-1843. https://doi.org/10.1039/P19870001841

[7] Vernin, G.(ed.). (1982). *Chemistry of heterocyclic compounds in flavours and aromas*, New York: Wiley & Sons.

[8] Richards, G.J., & Hill, J.P. (2021). The pyrazinacenes. *Acc. Chem. Res.*, *54*(16), 3228-3240. https://doi.org/10.1021/acs.accounts.1c00315

[9] Lown, J.W., Akhtar, M.H., & McDaniel, R.S. (1974). Stereochemistry and mechanism of the thermal [1,3] alkyl shift of stable 1,4-dialkyl-1,4-dihydropyrazines. *J. Org. Chem., 39*(14)*, 1998-2006.* https://doi.org/10.1021/jo00928a004

[10] Duan, X., Xin, H., & Yan, H. (2014). Design, synthesis, and biological evaluation of 1,4-diaryl-1,4-dihydropyrazines as novel 11*β*-HSD1 inhibitors. *Biol. Pharm. Bull., 37*(5), 840-846. https://doi.org/10.1248/bpb.b14-00070

[11] Ito, S., Takechi, H., Nakahara, K., Kashige, N., &Yamaguchi, T. (2010). Phenyl-substituted dihydropyrazines with DNA strand-breakage activity. *Chem. Pharm. Bull., 58*(6), 825-828. https://doi.org/10.1248/cpb.58.825

[12] Takechi, S., Yamaguchi, T., Nomura, H., Minematsu, T., Adachi, M., Kurata, H., & Kurata, R. (2006). Mutation spectrum induced by dihydropyrazines in *Escherichia coli*. *Biol. Pharm. Bull., 29*(1), 17-20. https://doi.org/10.1248/bpb.29.17. PMID: 16394502.

[13] Suresh, C.H., & Rakhi, R. (2016). A DFT study on dihydropyrazine annulated linear

polyacenes: aromaticity, stability and homo-lumo energy modulation. *Phys. Chem. Chem. Phys.*, *18*, 24631-24641. https://doi.org/10.1039/C6CP03723B

[14] Sun, C-L, Luo, X-E, Xu, H., Song, Q-W, Fan, Z-P, Wang, X-Z, Cao, J-J, Shi, Z-F, & Zhang, H-L. (2020). Aromaticity and tautomerism of a 4n π electron dihydrohexaazapentacene. *Org. Chem. Front*., *7*, 405-413. https://doi.org/10.1039/c9qo01285k

[15] Vlček, P., Havlas, Z., & Pavlíček, Z**.** (1999). Are 1,4-dihydropyrazines antiaromatic? *Ab initio* study of 1,4-dihydropyrazines and their tetrahydro derivatives. *Collect. Czech. Chem. Commun*., *64*, 633-648. https://doi.org/10.1135/cccc19990633

[16] Stewart, J.J.P. (1989). Optimization of parameters for semiempirical methods I. Method. *J. Comput. Chem*., *10*, 209-220. https://doi.org/10.1002/jcc.540100208

[17] Stewart, J.J.P. (1989). Optimization of parameters for semi empirical methods II. Application. *J. Comput. Chem., 10*, 221-264. https://doi.org/10.1002/jcc.540100209

[18] Leach, A.R. (1997). *Molecular modeling* (2nd ed.). Longman, Essex.

[19] Fletcher, P. (1990). *Practical methods of optimization* (1st ed.). New York: Wiley.

[20] Kohn, W., & Sham, L. (1965). Self-consistent equations including exchange and correlation effects. *J. Phys. Rev., 140*, 133-1138. https://doi.org/10.1103/PhysRev.140.A1133

[21] Parr, R.G., & Yang, W. (1989). *Density functional theory of atoms and molecules* (1st ed.). London: Oxford University Press.

[22] Cramer, C.J. (2004). *Essentials of computational chemistry* (2nd ed.). Chichester, West Sussex: Wiley.

[23] Becke, A.D. (1988). Density-functional exchange-energy approximation with correct asymptotic behavior. *Phys. Rev. A, 38*, 3098-3100. https://doi.org/10.1103/PhysRevA.38.3098

[24] Vosko, S.H., Wilk, L., & Nusair, M. (1980). Accurate spin-dependent electron liquid correlation energies for local spin density calculations: a critical analysis. *Can. J. Phys., 58*, 1200-1211. https://doi.org/10.1139/p80-159

[25] Lee, C., Yang, W., & Parr, R. G. (1988). Development of the Colle-Salvetti correlation energy formula into a functional of the electron density. *Phys. Rev., B, 37*, 785-789. https://doi.org/10.1103/PhysRevB.37.785

[26] PARTAN 06, Wavefunction Inc., Irvine CA, USA, 2006.

[27] Gaussian 03, Frisch, M.J., Trucks, G.W., Schlegel, H.B., Scuseria, G.E., Robb, M.A., Cheeseman, J.R., Montgomery, Jr., J.A., Vreven, T., Kudin, K.N., Burant, J.C., Millam, J.M., Iyengar, S.S., Tomasi, J., Barone, V., Mennucci, B., Cossi, M., Scalmani, G., Rega, N., Petersson, G.A., Nakatsuji, H., Hada, M., Ehara, M., Toyota, K., Fukuda, R., Hasegawa, J., Ishida, M., Nakajima, T., Honda, Y., Kitao, O., Nakai, H., Klene, M., Li, X., Knox, J.E., Hratchian, H.P., Cross, J.B., Bakken, V., Adamo, C., Jaramillo, J., Gomperts, R., Stratmann, R.E., Yazyev, O., Austin, A.J., Cammi, R., Pomelli, C., Ochterski, J.W., Ayala, P.Y., Morokuma, K., Voth, G.A., Salvador, P., Dannenberg, J.J., Zakrzewski, V.G., Dapprich, S., Daniels, A.D., Strain, M.C., Farkas, O., Malick, D.K., Rabuck, A.D., Raghavachari, K., Foresman, J.B., Ortiz, J.V., Cui, Q., Baboul, A.G., Clifford, S., Cioslowski, J., Stefanov, B.B., Liu, G., Liashenko, A., Piskorz, P., Komaromi, I., Martin, R.L., Fox, D.J., Keith, T., Al-Laham, M.A., Peng, C.Y., Nanayakkara, A., Challacombe, M., Gill, P.M.W., Johnson, B., Chen, W., Wong, M.W., Gonzalez, C., & Pople, J.A., Gaussian, Inc., Wallingford CT, 2004.

[28] Dewar, M.J.S., & Dougherty, R.C. (1975). *The PMO theory of organic chemistry*. New York: Plenum/Rosseta.

[29] Anbu, V., Vijayalakshmi, K.A., Karunathan, R., Stephen, A.D., & Nidhin, P.V. (2019). Explosives properties of high energetic trinitrophenyl nitramide molecules: A DFT and AIM analysis. *Arabian Journal of Chemistry*, *12*(5), 621-632. https://doi.org/10.1016/j.arabjc.2016.09.023

[30] Minkin, V.I., Glukhovtsev, M.N., & Simkin, B.Y. (1994). *Aromaticity and antiaromaticity: Electronic and structural aspects*. New York: Wiley.

[31] Schleyer, P.R., & Jiao, H. (1996). What is aromaticity?. *Pure Appl. Chem*., *68*, 209-218. https://doi.org/10.1351/pac199668020209

[32] Schleyer, P.R. (2001). Introduction: aromaticity. *Chem. Rev*., *101*, 1115-1118. https://doi.org/10.1021/cr0103221

[33] Cyranski, M.K., Krygowski, T.M., Katritzky, A.R., & Schleyer, P.R. (2002). To what extent can aromaticity be defined uniquely?. *J. Org. Chem*., *67*, 1333-1338. https://doi.org/10.1021/jo016255s

[34] Chen, Z., Wannere, C.S., Corminboeuf, C., Puchta, R., & Schleyer, P. von R. (2005). Nucleus independent chemical shifts (NICS) as an aromaticity criterion. *Chem. Rev*., *105*(10), 3842-3888. https://doi.org/10.1021/cr030088

[35] Gershoni-Poranne, R., & Stanger, A. (2015). Magnetic criteria of aromaticity. *Chem., Soc. Rev*., *44*(18), 6597-6615. https://doi.org/10.1039/C5CS00114E

[36] Dickens, T.K., & Mallion, R.B. (2016). Topological ring-currents in conjugated systems. *MATCH Commun. Math. Comput. Chem*., *76*, 297-356.

[37] Stanger, A. (2010). Obtaining relative induced ring currents quantitatively from NICS. *J. Org. Chem*., *75*(7), 2281-2288. https://doi.org/10.1021/jo1000753

[38] Monajjemi, M., & Mohammadian, N.T. (2015). S-NICS: An aromaticity criterion for nano molecules. *J. Comput. Theor. Nanosci*., *12*(11), 4895-4914. https://doi.org/10.1166/jctn.2015.4458

[39] Schleyer, P.R., Maerker, C., Dransfeld, A., Jiao, H., & Hommes, N.J.R.E. (1996). Nucleus independent chemical shifts: a simple and efficient aromaticity probe. *J. Am. Chem. Soc*., *118*, 6317-6318. https://doi.org/10.1021/ja960582d

[40] Corminboeuf, C., Heine, T., & Weber, J. (2003). Evaluation of aromaticity: A new dissected NICS model based on canonical orbitals. *Phys. Chem. Chem. Phys.*, *5*, 246-251. https://doi.org/10.1039/B209674A

[41] Stanger, A. **(**2006). Nucleus-independent chemical shifts (NICS): Distance dependence and revised criteria for aromaticity and antiaromaticity. *The Journal of Organic Chemistry*, *71*(3), 883-893. https://doi.org/10.1021/jo051746o

[42] Chen, Z., Wannere, C.S., Corminboeuf, C., Puchta, R., & Schleyer, P.R. (2005). Nucleus-independent chemical shifts (NICS) as an aromaticity criterion. *Chemical Reviews*, *105*(10), 3842-3888. https://doi.org/10.1021/cr030088+

[43] Reutov, O. (1970). *Theoretical principles of organic chemistry*. Moscow: Mir Pub.

[44] Anslyn, E.V., & Dougherty, D.A. (2006). *Modern physical organic chemistry*. Sausalito, California: University Science Books.

[45] Fleming, I. (1973). *Frontier orbitals and organic reactions*. London: Wiley.